THE JOURNAL OF PHYSICAL CHEMISTRY Letters

Letter

pubs.acs.org/JPCL

Infrared Spectra of Protonated Pyrene and Its Neutral Counterpart in Solid *para*-Hydrogen

Mohammed Bahou,[†] Yu-Jong Wu,*[,‡] and Yuan-Pern Lee*[,†,§]

[†]Department of Applied Chemistry and Institute of Molecular Science, National Chiao Tung University, 1001 Ta-Hsueh Road, Hsinchu 30010, Taiwan

[‡]National Synchrotron Radiation Research Center, 101 Hsin-Ann Road, Hsinchu 30076, Taiwan

[§]Institute of Atomic and Molecular Sciences, Academia Sinica, Taipei 10617, Taiwan

Supporting Information

ABSTRACT: Protonated polycyclic aromatic hydrocarbons (H^+PAHs) have been reported to have infrared (IR) bands at wavenumbers near those of unidentified infrared (UIR) emission bands from interstellar objects. We produced 1-$C_{16}H_{11}^+$ and 1-$C_{16}H_{11}$ upon electron bombardment during matrix deposition of *p*-H_2 containing pyrene ($C_{16}H_{10}$) in a small proportion. Intensities of absorption features of 1-$C_{16}H_{11}^+$ decreased after the matrix was maintained in darkness or irradiated with light at 365 nm, whereas those of 1-$C_{16}H_{11}$ increased. The observed line wavenumbers and relative intensities of 1-$C_{16}H_{11}^+$ and 1-$C_{16}H_{11}$ agree satisfactorily with the scaled vibrational wavenumbers and IR intensities predicted with the B3PW91/6-311++G(2d,2p) method. Our method, being relatively clean with negligible fragmentation, is applicable to larger H^+PAH; it has the advantages of producing excellent IR spectra covering a broad spectral range with narrow lines and accurate intensities, so that structural identification among various isomers is feasible.

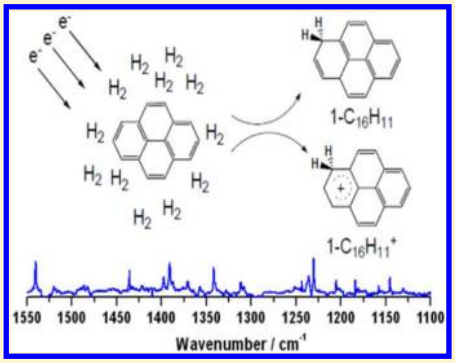

SECTION: Spectroscopy, Photochemistry, and Excited States

The infrared emission spectra of galactic and extragalactic objects show features at 3.3, 6.2, 7.7, 8.6, and 11.2 μm, the so-called unidentified interstellar infrared (UIR) bands. These features are generally attributed to polycyclic aromatic hydrocarbons (PAHs) and their derivatives,[1] even though no definitive PAH responsible for the UIR bands has been positively identified. Because proton sources are abundant in space, protonated PAHs, designated as H^+PAHs, are expected to be likewise abundant. Furthermore, because H^+PAHs are stable closed-shell molecules, they become effective candidates for carriers of the UIR bands from the perspective of interstellar chemistry.[2] Laboratory experiments have demonstrated that H^+PAHs are formed readily through protonation of PAH or attachment of a H atom to PAH^+ cations.[3] Comparisons of the astronomical spectra with those of various H^+PAHs obtained from experiments or theory support the hypothesis that H^+PAHs are possible carriers of the UIR and the diffuse interstellar bands (DIBs).[3−6] Although UIR bands from various objects are similar, detailed investigations have revealed significant variations in peak position and relative intensities of these bands from one source to another. Hence, the characterization of the infrared (IR) spectrum of individual H^+PAHs is important in understanding these variations.

Recording IR spectra of H^+PAHs in laboratories is challenging, largely because of the difficulties in generating H^+PAHs in sufficient quantity for spectral interrogation. Two major spectral methods are employed to yield IR spectra of H^+PAH. One employs IR multiphoton dissociation (IRMPD) of H^+PAH on monitoring the loss of either the H atom or H_2 molecule with an ion cyclotron resonance mass spectrometer.[5,7−9] Another method measures the single-photon IR photodissociation (IRPD) action spectra of cold H^+PAH tagged with a weakly bound ligand, such as Ar, by monitoring the loss of the ligand.[10−12] Because of the small perturbation by Ar, the action spectrum of the Ar-tagged H^+PAH is similar to the IR spectrum of the bare cation. Although the Ar tagging IRPD method provides much improved spectra over those from IRMPD, a critical limitation of the Ar tagging method is its difficulty in tagging large protonated PAHs because of their large internal energy. So far, the largest protonated species detected with this method is protonated naphthalene.[12] According to an astrochemical model, PAH molecules containing 20−80 carbon atoms are photochemically more stable in interstellar clouds.[1] Hence, a new method for investigating the IR spectra of the large protonated PAHs with high spectral resolution is essential.

Pyrene ($C_{16}H_{10}$), the smallest peri-condensed PAH, comprises four benzenoid rings. Five distinct sites of pyrene are possible for protonation or hydrogenation,[13,14] as shown in

Received: May 2, 2013
Accepted: May 28, 2013
Published: May 28, 2013

 © 2013 American Chemical Society dx.doi.org/10.1021/jz400923k | *J. Phys. Chem. Lett.* 2013, 4, 1989−1993

Figure 1. The most stable isomer of protonated pyrene is predicted to be 1-$C_{16}H_{11}^+$, followed by 4-$C_{16}H_{11}^+$ (43), 2-

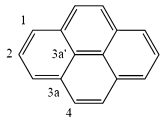

Figure 1. Possible sites for protonation or hydrogenation of pyrene.

$C_{16}H_{11}^+$ (59), 3a′-$C_{16}H_{11}^+$ (108), and 3a-$C_{16}H_{11}^+$ (111); the energies in kJ mol^{-1} relative to that of 1-$C_{16}H_{11}^+$ are listed in parentheses. Dopfer recorded the only available IR spectrum of $C_{16}H_{11}^+$ with the IRMPD technique.[5] Several overlapping broad features were reported in the region of 600−1800 cm^{-1}, but no information about the protonation site was provided. Garkusha et al. recorded the electronic absorption spectra[15] of 1-$C_{16}H_{11}^+$ and 1-$C_{16}H_{11}$ and the dispersed fluorescence spectrum[16] of 1-$C_{16}H_{11}^+$ in neon matrixes. Vibrational wavenumbers of 20 modes of the X $^1A'$ state of 1-$C_{16}H_{11}^+$ were determined by comparison with vibrational wavenumbers predicted using the B3LYP/cc-pVDZ method. No IR spectrum of $C_{16}H_{11}$ has been reported.

A new method for investigating IR spectra of H^+PAHs and their neutral counterparts was developed using electron bombardment during *p*-H_2 matrix deposition. With this technique, we have obtained high-resolution IR spectra of protonated benzene ($C_6H_7^+$)[17] and naphthalene (*α*- and *β*-$C_{10}H_9^+$),[18] as well as their neutral counterparts. We demonstrated that this method produces mainly the protonated parent and its neutrals without fragmentation; the IR spectra showed small widths and an excellent signal-to-noise ratio with wide spectral coverage. To demonstrate that this method is applicable also to larger PAHs, we extended it to investigate protonated pyrene as the first step.

A partial IR spectrum of a $C_{16}H_{10}$/*p*-H_2 (1/1500) matrix bombarded with electrons during deposition is shown in Figure 2A. Absorption features of pyrene, marked P in the figure, and other features were observed; spectra covering a wider spectral range are available in Figures S1 and S2 in the Supporting Information. To distinguish these features, we irradiated the matrix at 365 nm and plotted the difference spectrum, obtained upon subtraction of the spectrum recorded before irradiation from that recorded after irradiation, in Figure 2B; lines pointing upward indicate production, whereas those pointing downward indicate destruction. Irradiation of the matrix with UV light is expected to release electrons trapped in the matrix, resulting in the neutralization of cations.[17,18] Without irradiation, the trapped electrons diffuse slowly and might also recombine with the cations to form neutral species. In a separate experiment, we maintained the matrix in darkness for 20 h and plotted the difference spectrum in Figure 2C. The spectrum is similar to that recorded upon UV irradiation but with smaller changes in the intensities of most lines.

The observed features in Figure 2B and C are classified into four groups according to the correlated changes in intensity at various stages of the experiment. Most downward features, designated as A^+, with intense lines at 1618.0, 1540.2, 1391.3, 1230.2, and 868.9 cm^{-1} are likely associated with a cationic species because of its reaction with electrons in *p*-H_2; they are assigned to 1-$C_{16}H_{11}^+$, to be discussed later. Some downward features are due to loss of pyrene, marked P; some of them show first-derivative shape because of a small shift in the line positions of pyrene in two spectra. Three upward lines at 1531.0, 1295.0, and 1232.9 cm^{-1}, marked as P^-, are readily assigned to $C_{16}H_{10}^-$ upon comparison with reported values of 1529, 1294, and 1234 cm^{-1}.[19] Because pyrene has a small positive electron affinity (0.41 eV),[20] $C_{16}H_{10}^-$ is readily produced from reaction of pyrene with electrons. Most other upward features with intense lines at 1552.3, 839.7, 811.8, and 654.4 cm^{-1}, designated as A, are likely associated with the neutral species; they are assigned to 1-$C_{16}H_{11}$, to be discussed later.

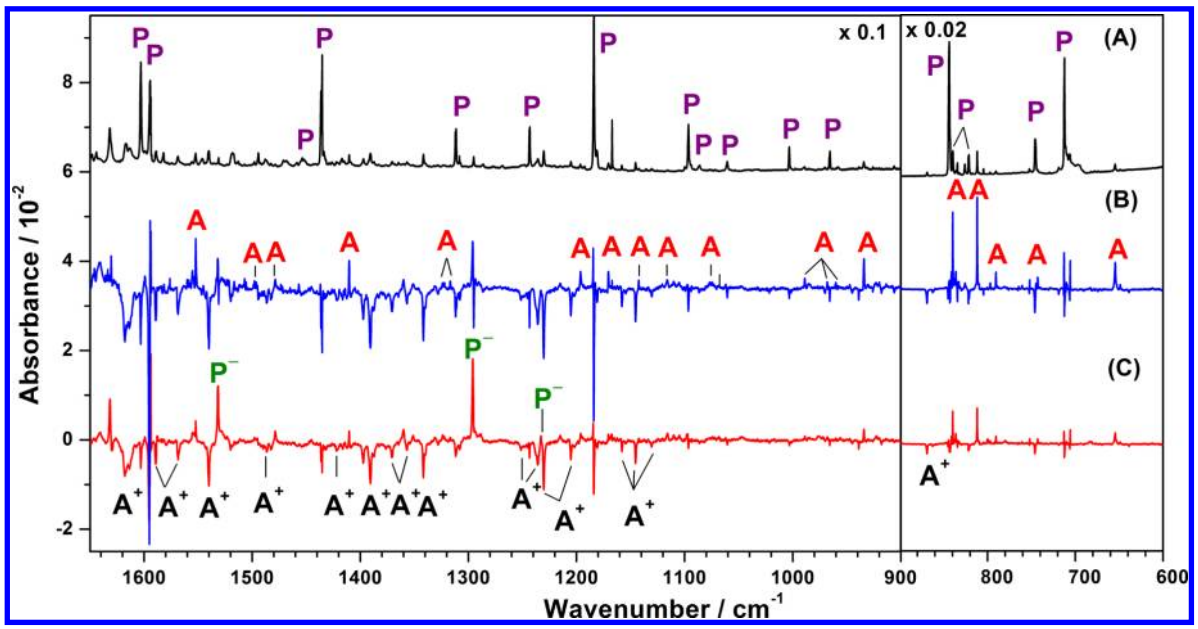

Figure 2. Partial IR spectra of (A) electron-bombarded $C_{16}H_{10}$/*p*-H_2 (1/1500), (B) difference spectrum of the matrix sample upon irradiation at 365 nm for 2.5 h, and (C) difference spectrum of another $C_{16}H_{10}$/*p*-H_2 (1/1500) matrix after maintaining in darkness for 20 h. P: $C_{16}H_{10}$; P^-: $C_{16}H_{10}^-$; A^+: 1-$C_{16}H_{11}^+$; A: 1-$C_{16}H_{11}$.

dx.doi.org/10.1021/jz400923k | *J. Phys. Chem. Lett.* 2013, 4, 1989−1993

In Figure 3B, we inverted Figure 2B and indicate lines in group A^+ with arrows; regions due to interference of $C_{16}H_{10}$ and $C_{16}H_{10}^-$ are shaded in light gray. In Figure 3C–E, we compare the spectra of 1-$C_{16}H_{11}^+$, 2-$C_{16}H_{11}^+$, and 4-$C_{16}H_{11}^+$, simulated according to scaled vibrational wavenumbers and IR intensities predicted with the B3PW91/6-311++G(2d,2p) method. Calculated vibrational wavenumbers and IR intensities of the three low-energy isomers of $C_{16}H_{11}^+$ and their neutrals are available in Tables S1–S4 (Supporting Information). The scaling factors 0.958 and 0.982 for the CH stretching and all other modes, respectively, were derived upon comparing the observed wavenumbers of pyrene in the *p*-H_2 matrix with the calculated wavenumbers. The spectral patterns of these isomers are distinct in the region of 1100–1650 cm^{-1} because of dissimilar bonding effects on the aromatic rings when the protonation site varies. The best agreement between experiments and prediction in terms of relative intensities and positions is obtained for 1-$C_{16}H_{11}^+$. Some representative lines of A^+ are compared with theoretical calculations and fluorescence in Table 1. A complete list is available in Table S1 (Supporting Information). Spectra covering a wider spectral range are shown in Figure S3 (Supporting Information).

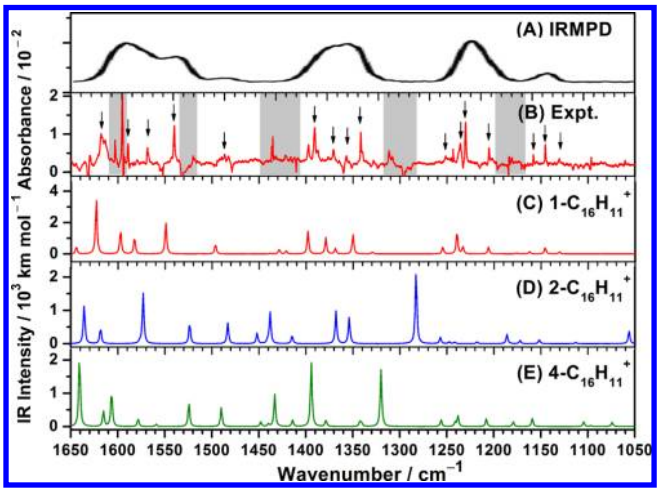

Figure 3. Comparison of observed with predicted IR spectra of $C_{16}H_{11}^+$. (A) spectrum of $C_{16}H_{11}^+$ recorded with the IRMPD method,[5] (B) spectrum of lines in group A^+ (indicated with ↓), taken from Figure 2B and inverted, and (C–E) spectra of 1-$C_{16}H_{11}^+$, 2-$C_{16}H_{11}^+$, and 4-$C_{16}H_{11}^+$ simulated according to scaled calculated vibrational wavenumbers and IR intensities.

The deviations between observed and predicted vibrational wavenumbers are within 24 cm^{-1} (0.9%), and almost all features predicted with an IR intensity greater than 8 km mol^{-1} in the probed spectral region were observed. Intense lines predicted near 1623 and 1549 cm^{-1} for CC stretching modes are observed at 1618.0 and 1540.2 cm^{-1}. The CH_2 scissoring mode predicted at 1350 cm^{-1} is observed at 1341.7 cm^{-1}, but the CH_2 symmetric stretching mode predicted at 2880 cm^{-1} is too weak to be positively identified. Similar bands of CH_2 scissor were also observed at 1292.4 and 1265.6 cm^{-1} for 1-$C_{10}H_9^+$ and 2-$C_{10}H_9^+$, respectively.[18]

Many observed intense IR-active modes are unobserved in fluorescence,[16] presumably because of poor Franck–Condon overlap in fluorescence. The mode assignments in fluorescence were made based on comparison of the observed spacing from the transition origin and predicted wavenumbers without information on the intensity. The spectrum of $C_{16}H_{11}^+$ obtained from IRMPD[5] is reproduced in Figure 3A. The reported broad features in IRMPD are in satisfactory agreement with those recorded in this work except for red shifts due to anharmonic effects in multiphoton absorption. As our spectral resolution is much superior, we identify unambiguously 1-$C_{16}H_{11}^+$, the most stable isomer of $C_{16}H_{11}^+$, as the structure associated with the observed lines.

Table 1. Comparison of Vibrational Wavenumbers and Relative IR Intensities of Representative Lines[a] of 1-$C_{16}H_{11}^+$

B3PW91[b]/6-311++G(2d,2p)	IR/*p*-H_2	LIF/Ne[c]	mode description
1623 (100)[d]	1618.0 (100)[d]	1619	CC stretch
1549 (58)	1540.2 (41)		CC stretch
1398 (40)	1391.3 (46)		ring deform
1350 (36)	1341.7 (31)		CH_2 scissor
1240 (41)	1230.2 (38)	1230?	in-plane CH bend
872 (30)	868.9 (29)		out-of-plane CH bend

[a]A complete list is available in Table S1 (Supporting Information). [b]Scaled; see text. [c]Fluorescence data from ref 16. [d]Relative intensities are listed in parentheses. The calculated maximal IR intensity is 257.6 km mol^{-1}.

In Figure 4A, we show the difference spectrum of the matrix upon irradiation at 365 nm; lines associated with group A are indicated with arrows and regions due to interference of $C_{16}H_{10}$ and $C_{16}H_{10}^-$ are shaded in light gray. Lines in group A are likely correlated with the most stable neutral form (1-$C_{16}H_{11}$) because conversion from lines in group A^+ (1-$C_{16}H_{11}^+$) to group A was observed upon irradiation or upon maintaining the matrix in darkness. In Figure 4B–D, we compare the spectra of 1-$C_{16}H_{11}$, 2-$C_{16}H_{11}$, and 4-$C_{16}H_{11}$, simulated according to scaled vibrational frequencies and IR intensities predicted with the B3PW91/6-311++G(2d,2p) method. The best agreement with experiments in terms of relative intensities and positions is obtained for the predicted spectrum of 1-$C_{16}H_{11}$. The predicted spectra of other candidates disagree with the observed spectrum. Vibrational wavenumbers and relative IR intensities of representative lines of group A observed in this work are compared with theoretical calculations in Table 2. A complete

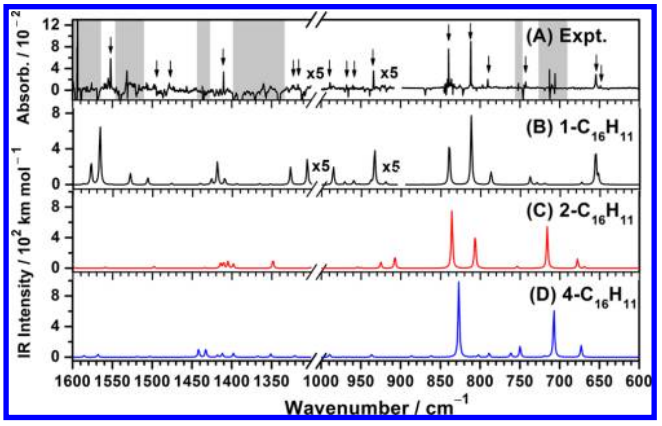

Figure 4. Comparison of observed and predicted IR spectra of $C_{16}H_{11}$. (A) Spectrum of lines in group A (indicated with ↓), taken from Figure 2B, and (B–D) spectra of 1-$C_{16}H_{11}$, 2-$C_{16}H_{11}$, and 4-$C_{16}H_{11}$ simulated according to calculated scaled vibrational wavenumbers and IR intensities.

dx.doi.org/10.1021/jz400923k | J. Phys. Chem. Lett. 2013, 4, 1989–1993

Table 2. Comparison of Vibrational Wavenumbers and Relative IR Intensities of Representative Lines[a] of 1-$C_{16}H_{11}$

B3PW91[b]/6-311++G(2d,2p)	IR/*p*-H_2	mode description[c]
2856 (61)[d]	2839.7 (20)[d]	CH_2 sym. stretch
1566 (29)	1552.3 (33)	CC stretch
1419 (12)	1410.3 (13)	CH_2 scissor
839 (67)	839.7 (42)	oop CH bend
812 (100)	811.8 (100)	oop CH bend
656 (52)	654.4 (61)	oop CH bend + CH_2 rock

[a]A complete list is available in Table S3 (Supporting Information). [b]Scaled; see text. [c]oop: out-of-plane. [d]Relative intensities are listed in parentheses. The calculated IR intensity of the 812 cm^{-1} line is 56.5 km mol^{-1}.

list is available in Table S3 (Supporting Information). Spectra covering a wider spectral range are shown in Figure S4 (Supporting Information). Taking into account all available information, we assign the features in group A to 1-$C_{16}H_{11}$.

The observed vibrational wavenumbers of 1-$C_{16}H_{11}$ deviate from those predicted by <22 cm^{-1} (1.3%); almost all features with an IR intensity greater than 3 km mol^{-1} in the probed region were observed. Intense lines predicted at 839, 812, and 656 cm^{-1} and observed at 839.7, 811.8, and 654.4 cm^{-1} are attributed to out-of-plane CH bending modes, with the latter mixed with the CH_2 rocking mode. The characteristic absorption of the CH_2 symmetric stretching mode was observed at 2839.7 cm^{-1}.

The reported IRMPD bands of protonated pyrene are similar to those of protonated coronene, which show satisfactory agreement with the UIR emission bands.[5] Although the absorption spectra might differ from the emission spectra,[21,22] our spectra with improved resolution and true IR absorption intensity provide some basis for comparison with the UIR bands; the spectral shifts caused by the perturbation of the *p*-H_2 matrix are typically <1%. The most intense line of 1-$C_{16}H_{11}^+$ observed at 1618.0 cm^{-1} (6.18 μm) and two weaker ones at 1588.9 (6.29 μm) and 1568.7 cm^{-1} (6.37 μm) match well with those of the UIR band at 6.2 μm; these features, correlated with the distortion of the carbon ring having the charge in the π-system, were also found in protonated naphthalene.[12,18] The corresponding unique features in UIR might be a special consequence of protonation. The two additional lines at 1341.7 (7.45 μm, CH_2 scissor) and 868.9 cm^{-1} (11.5 μm, CH out-of-plane bend) also agree satisfactorily with those of UIR bands near 7.6 and 11.2 μm, supporting that larger protonated PAH cations have the required chromophores to explain many of the prominent features of the UIR. However, the line at 1540.2 cm^{-1} (6.49 μm) for the ring distortion mode seems too intense for the edge of the UIR band near 6.2 μm, suggesting that 1-$C_{16}H_{11}^+$ is unlikely the major carrier of the UIR. For 1-$C_{16}H_{11}$, the lines at 3046.6 and 3044.6 cm^{-1} (3.28 μm) and the most intense one at 811.8 cm^{-1} (12.3 μm) match well with those of the UIR band at 3.3 and 12.7 μm, respectively, but lines at 839.7 (11.9 μm) and 654.4 cm^{-1} (15.3 μm) correspond to no UIR band with significant intensities.

Our results clearly indicate that 1-$C_{16}H_{11}$ and 1-$C_{16}H_{11}^+$ are the major products upon electron bombardment during deposition of a mixture of $C_{16}H_{10}$ and *p*-H_2, enabling us to record their IR spectra with much improved resolution and range of spectral coverage. This "clean" method provides a direct structural characterization of the H^+PAH and its neutral species that is applicable to larger H^+PAH. Although 1-$C_{16}H_{11}^+$ has the required chromophores to explain many of the prominent features of the UIR, our data indicate that it is unlikely the major carrier of the interstellar unidentified infrared emission bands.

EXPERIMENTAL SECTION

IR absorption spectra covering the spectral range of 450−5000 cm^{-1} were recorded with an interferometric spectrometer (Bomen DA8) equipped with a KBr beamsplitter and a Hg−Cd−Te detector cooled to 77 K. Typically, 600 scans at a resolution of 0.25 cm^{-1} were recorded at each stage of an experiment.[23]

The $C_{16}H_{11}^+$ cation and $C_{16}H_{11}$ were produced upon electron bombardment of a gaseous sample during deposition of *p*-H_2 containing $C_{16}H_{10}$ in a small proportion. An electron beam at 300 eV with a current of 70 μA was generated with an electron gun (Kimball Physics, Model EFG-7). Electron bombardment of *p*-H_2 produces H_2^+ that further reacts with H_2 to produce H_3^+ and H. $C_{16}H_{11}^+$ is presumed to have been produced upon proton transfer from H_3^+, and $C_{16}H_{11}$ was produced upon either neutralization of $C_{16}H_{11}^+$ or reaction of $C_{16}H_{11}$ with H. Typically, a gaseous mixture of $C_{16}H_{10}$/*p*-H_2 (1/1000−1/3000) was deposited over a period of 5−17 h with a flow rate of 10−13 mmol h^{-1}. Photoirradiation experiments were performed with a light-emitting diode (375 mW) with emission at 365 ± 10 nm. Normal H_2 (99.9999%, Scott Specialty Gases) was passed through a trap at 77 K before entering the *p*-H_2 converter that comprised a copper cell filled with iron(III) oxide catalyst (Aldrich) and cooled with a closed-cycle refrigerator (Advanced Research Systems, DE204AF). The conversion efficiency was controlled by the temperature of the catalyst; at a temperature of 11−13 K, *o*-H_2 is less than 100 ppm. Pyrene (99.8%, Aldrich) was heated to 328 K to increase its vapor pressure during deposition.

Energies, equilibrium structures, vibrational wavenumbers, and IR intensities were calculated with the Gaussian 09 program.[24] Density functional theory (DFT) calculations were performed using the B3PW91 method with Becke's three-parameter hybrid exchange functional[25] and an exchange functional of Perdew and Wang as the correlation functional.[26] The standard basis set 6-311++G(2d,2p) was used. The scaling factors 0.958 and 0.982 for the CH stretching modes and all other modes, respectively, were derived upon comparing the observed wavenumbers of pyrene in the *p*-H_2 matrix with the calculated wavenumbers.

ASSOCIATED CONTENT

Supporting Information

The calculated and experimental vibrational wavenumbers and infrared intensities of all species, and spectra with wider spectral coverage (Tables S1−S4 and Figures S1−S4). This material is available free of charge via the Internet at http://pubs.acs.org.

AUTHOR INFORMATION

Corresponding Author

*E-mail: yjwu@nsrrc.org.tw (Y.-J.W.); yplee@mail.nctu.edu.tw (Y.-P.L.).

Notes

The authors declare no competing financial interest.

■ ACKNOWLEDGMENTS

National Science Council (Grants NSC101-2745-M009-001-ASP and NSC101-2113-M-213-002) and the Ministry of Education, Taiwan ("ATU Plan" of National Chiao Tung University) supported this work. The National Center for High-Performance Computing provided computer time.

■ REFERENCES

(1) Peeters, E. Astronomic Observations of the PAH Emission Bands. In *PAHs and the Universe*; Joblin, C., Tielens, A. G. G. M., Eds.; EAS Publication Series 46; Cambridge University Press: France, 2011; pp 13−27.

(2) Snow, T. P.; Le Page, V.; Keheyan, Y.; Bierbaum, V. M. The Interstellar Chemistry of PAH Cations. *Nature* **1998**, *391*, 259−260.

(3) Le Page, V.; Keheyan, Y.; Bierbaum, V. M.; Snow, T. P. Chemical Constraints on Organic Cations in the Interstellar Medium. *J. Am. Chem. Soc.* **1997**, *119*, 8373−8374.

(4) Pathak, A.; Sarre, P. J. Protonated PAHs as Carriers of Diffuse Interstellar Bands. *Mon. Not. R. Astron. Soc.* **2008**, *391*, L10−L14.

(5) Dopfer, O. Laboratory Spectroscopy of Protonated PAH Molecules Relevant for Interstellar Chemistry. In *PAHs and the Universe*; Joblin, C., Tielens, A. G. G. M., Eds.; EAS Publication Series 46; Cambridge University Press: France, 2011; pp 103−108.

(6) Hammonds, M.; Pathak, A.; Sarre, P. J. TD-DFT Calculations of Electronic Spectra of Hydrogenated Protonated Polycyclic Aromatic Hydrocarbon (PAH) Molecules: Implication for the Origin of the Diffuse Interstellar Bands? *Phys. Chem. Chem. Phys.* **2009**, *11*, 4458−4464.

(7) Jones, W.; Boissel, P.; Chiavarino, B.; Crestoni, M. E.; Fornarini, S.; Lemaire, J.; Maitre, P. Infrared Fingerprint of Protonated Benzene in the Gas Phase. *Angew. Chem., Int. Ed.* **2003**, *42*, 2057−2059.

(8) Dopfer, O.; Solca, N.; Lemaire, J.; Maitre, P.; Crestoni, M. E.; Fornarini, S. Protonation Sites of Isolated Fluorobenzene Revealed by IR Spectroscopy in the Fingerprint Range. *J. Phys. Chem. A* **2005**, *109*, 7881−7887.

(9) Knorke, H.; Langer, J.; Oomens, J.; Dopfer, O. Infrared Spectra of Isolated Protonated Polycyclic Aromatic Hydrocarbon Molecules. *Astrophys. J. Lett.* **2009**, *706*, L66−L70.

(10) Solca, N.; Dopfer, O. Protonated Benzene: IR Spectrum and Structure of $C_6H_7^+$. *Angew. Chem., Int. Ed.* **2002**, *41*, 3628−3631.

(11) Douberly, G. E.; Ricks, A. M.; Schleyer, P. v. R.; Duncan, M. A. Infrared Spectroscopy of Gas Phase Benzenium Ions: Protonated Benzene and Protonated Toluene from 750 to 3400 cm^{-1}. *J. Phys. Chem. A* **2008**, *112*, 4869−4874.

(12) Ricks, A. M.; Douberly, G. E.; Duncan, M. A. The Infrared Spectrum of Protonated Naphthalene and Its Relevance for the Unidentified Infrared Emission Bands. *Astrophys. J.* **2009**, *702*, 301−306.

(13) Rasmussen, J. A.; Henkelman, G.; Hammer, B. Pyrene: Hydrogenation, Hydrogen Evolution, and π-Band Model. *J. Chem. Phys.* **2011**, *134*, 164703/1−164703/10.

(14) Calvo, F.; Basire, M.; Parneix, P. Temperature Effects on the Rovibrational Spectra of Pyrene-Based PAHs. *J. Phys. Chem. A* **2011**, *115*, 8845−8854.

(15) Garkusha, I.; Fulara, J.; Sarre, P. J.; Maier, J. P. Electronic Absorption Spectra of Protonated Pyrene and Coronene in Neon Matrixes. *J. Phys. Chem. A* **2011**, *115*, 10972−10978.

(16) Garkusha, I.; Fulara, J.; Maier, J. P. Fluorescence of Protonated Pyrene and Coronene in Neon Matrices. *J. Mol. Struct.* **2012**, *1025*, 147−150.

(17) Bahou, M.; Wu, Y.-J.; Lee, Y.-P. A New Method for Investigating Infrared Spectra of Protonated Benzene ($C_6H_7^+$) and Cyclohexadienyl Radical (C_6H_7) Using Para-Hydrogen. *J. Chem. Phys.* **2012**, *136*, 154304/1−154304/8.

(18) Bahou, M.; Wu, Y.-J.; Lee, Y.-P. Formation and Infrared Absorption of Protonated Naphthalene (1-$C_{10}H_9^+$ and 2-$C_{10}H_9^+$) and Their Neutral Counterparts in Solid Para-Hydrogen. *Phys. Chem. Chem. Phys.* **2013**, *15*, 1907−1917.

(19) Foley, J. K.; Korzeniewski, C.; Pons, S. Anodic and Cathodic Reactions in Acetonitrileltetra-n-butylammonium Tetrafluoroborate: An Electrochemical and Infrared Spectroelectrochemical Study. *Can. J. Chem.* **1988**, *66*, 201−206.

(20) Ando, N.; Kokubo, S.; Mitsui, M.; Nakajima, A. Photoelectron Spectroscopy of Pyrene Cluster Anions, $(pyrene)_n^-$ (n=1−20). *Chem. Phys. Lett.* **2004**, *389*, 279−283.

(21) Kim, H. S.; Saykally, R. J. Single-Photon Infrared Emission Spectroscopy of Gaseous Polycyclic Aromatic Hydrocarbon Cations: A Direct Test for Proposed Carriers of the Unidentified Infrared Emission Bands. *Astrophys. J. Suppl. Ser.* **2002**, *143*, 455−467.

(22) Schlemmer, S.; Cook, D. J.; Harrison, J. A.; Wurfel, B.; Chapman, W.; Saykally, R. J. The Unidentified Interstellar Infrared Bands: PAHs as Carriers? *Science* **1994**, *265*, 1686−1689.

(23) Lee, Y.-P.; Wu, Y.-J.; Lees, R. M.; Xu, L.-H.; Hougen, J. T. Internal Rotation and Nuclear Spin Conversion of CH_3OH in Solid Parahydrogen. *Science* **2006**, *311*, 365−368.

(24) Frisch, M. J.; Trucks, G. W.; Schlegel, H. B.; Scuseria, G. E.; Robb, M. A.; Cheeseman, J. R.; Scalmani, G.; Barone, V.; Mennucci, B.; Petersson, G. A.; et al. *GAUSSIAN 09*, revision A.02; Gaussian, Inc.: Wallingford, CT, 2009.

(25) Becke, A. D. Density-Functional Thermochemistry. III. The Role of Exact Exchange. *J. Chem. Phys.* **1993**, *98*, 5648−5652.

(26) Perdew, J. P.; Burke, K.; Wang, Y. Generalized Gradient Approximation for the Exchange−Correlation Hole of a Many-Electron System. *Phys. Rev. B* **1996**, *54*, 16533−16539.